Thermodynamic and Kinetic Study of the Interactions of Ni(II) with FMN and FAD

Joseph Bidwell, Jean Thomas, and John Stuehr*

Contribution from the Department of Chemistry, Case Western Reserve University, Cleveland, Ohio 44106. *Received April 17, 1985*

Abstract: A thermodynamic and temperature-jump kinetic study has been carried out for the interactions of Ni(II) with the coenzymes flavin adenine mononucleotide (FMN) and flavin adenine dinucleotide (FAD) at 15 °C and $I = 0.1$ M. For the former, *two* relaxation times ($\sim 10^{-3}$ and 10^{-4} s) were characterized as a function of concentration and pH. These were attributed to the formation of nickel phosphate and nickel phosphate–adenine (back-bound) complexes, respectively. For the NiFAD system, *four* distinct relaxation times were observed, which ranged from about 100 μs to 35 ms. These were interpreted on the basis of a multistep complexation mechanism involving the initial interaction of Ni(II) with the phosphate moiety, followed by a sequence of back-bound complexes involving interactions with the adenine and isoalloxazine ring systems. The nickel phosphate interactions were kinetically consistent with solvent exchange rates from the primary coordination sphere of Ni(II). To the best of our knowledge, the NiFAD system is the only one for which four relaxation times have been observed and characterized.

The coenzymes flavin mononucleotide (FMN, also known as riboflavin phosphate) and flavin adenine dinucleotide (FAD), are involved in a wide variety of biological oxidation–reduction reactions.[1] Many flavoenzymes contain metal ions, e.g., molybdenum, iron, and zinc, at or near the active site.[2-4] Physical studies have failed to establish whether a direct metal–flavin contact occurs in any biological system, although there has been considerable speculation that such exists.[5-11]

Recent studies have employed model systems in an attempt to characterize the postulated metal–flavin contact.[12-14] The emphasis of that research has been on the metal–isoalloxazine ring system to the exclusion of phosphate or other interactions. Before meaningful model systems can be employed, however, the fundamental interactions between the coenzymes themselves and various metal ions need to be elucidated.[15]

We report in this paper the first rapid kinetic study of the mechanism of divalent metal ion interactions with the coenzymes FMN and FAD. The two compounds are structurally related to each other as well as to other coenzymes and phosphates that we have previously reported on.[16] FAD for example, is structurally a combination of FMN and adenosine monophosphate (AMP5′), as shown in Figure 1.

Table I. pK and Stability Constants for the Ni^{II}FMN and Ni^{II}FAD Systems[a,b]

	pK_{a1}	pK_{a2}	K_{ML}, M^{-1}	K_{MHL},[d] M^{-1}
FMN	2.05	6.22	118	5.7
	(1.89)[c]	(6.37)[c]		
FAD	2.06	3.69	250[e]	

[a] At 15 °C, 0.1 M KNO_3. [b] Both ligands have a third pK of about 10.3. [c] At 35 °C. Taqui Khan, M. M.; Mohan, M. S. *J. Inorg. Nucl. Chem.* **1973**, *35*, 1749. [d] Complex with the secondary phosphate protonated. [e] See text.

Ni(II) was chosen as the metal ion for these studies because of the large body of kinetic information that is already available for that ion.[16] It therefore serves as a useful representative of divalent transition-metal ion interactions with these and related coenzymes.

Experimental Section

Materials. Sodium salts of FAD and FMN of the highest available purity were obtained from Sigma Chemical Co. Solutions were prepared daily and protected from light; purity was verified by HPLC.[17] Stock solutions of Ni(II) were prepared from reagent-grade nitrate (Baker) and standardized either spectrophotometrically or via EDTA titration.

Methods: Equilibrium Constants. The pK_a's of FMN and FAD and stability constants of NiFMN complexes were determined by potentiometric titration[18] with 0.1 M carbonate-free KOH in 0.1 M KNO_3. For the determination of metal ion binding constants, titrations were carried out in the presence of Ni(II) (1:1 or 1:2 metal–ligand ratios) in conjunction with a Corning 101 digital pH electrometer calibrated with Beckman pH 4 and 7 buffers.

Kinetics. The kinetic experiments were carried out at 15 °C and $I =$ 0.1 M KNO_3 on a temperature-jump spectrometer (Messanlagan Studiengesellschaft).[19] A precooled solution was added to the thermostated T-jump cell and equilibrated to 10 °C. The discharge of 30 kV through the system yielded a temperature rise of 5 °C within a few microseconds. The relaxation effects of the system were monitored via transmittance changes, stored on a Biomation 802 transient recorder, and displayed on an oscilloscope screen. A Polaroid photograph of the trace was analyzed for the relaxation time.

The various relaxation processes were followed with and without pH indicators. FMN exhibits a strong absorption in the visible part of the spectrum, so that the reactions could be followed either at ~500 nm without an indicator or with a pH indicator (bromocresol purple, pK_{In} = 6.3 or chlorophenol red, pK_{In} = 6.0) at ~590 nm.[20] For FAD, the

(1) Walsh, C. *Acc. Chem. Res.* **1980**, *13*, 148.
(2) Bray, R. C. In "The Enzymes"; Boyer, P. D., Ed.; Academic Press: New York, 1975; pp 229 ff.
(3) Singer, T. P.; Gregolin, C. *Biochim. Biophys. Acta* **1963**, *67*, 201.
(4) Singer, T. P.; Cremona, T. J. *Biol. Chem.* **1964**, *239*, 1466.
(5) Mahler, H. R.; Fairhurst, A. S.; Mackler, B. *J. Am. Chem. Soc.* **1955**, *77*, 1514.
(6) Hemmerich, P. In "Bioinorganic Chemistry"; Raymond, K. N., Ed.; American Chemical Society: Washington, DC, 1977; Vol. II, pp 312 ff.
(7) Hemmerich, P.; Lauterwin, J. In "Inorganic Biochemistry", Eichhorn, G. L., Ed.; Elsevier: Amsterdam, 1973; Vol. 2, 1168.
(8) Steenkamp, D. J.; Singer, T. P.; Beinert, H. *Biochem. J.* **1978**, *169*, 361.
(9) Rajagopalan, K. U.; Hendler, P.; Palmer, G.; Beinert, H. *J. Biol. Chem.* **1968**, *243*, 3797.
(10) Beinert, H.; Kenney, W. C.; Singer, T. P.; Steenkamp, D. In Flavins and Flavoproteins; "Proceedings of the 6th International Symposium on Flavins and Flavoproteins"; Yagi, K., Yamono, T., Eds., University Park Press: Baltimore, 1980; pp 283 ff.
(11) Mahler, H. R.; Green, D. E. *Science (Washington, D.C.)* **1954**, *120*, 7.
(12) Clarke, M. J.; Brennon, T. F.; Garafalo, A. R.; Dowling, M. G. *J. Biol. Chem.* **1980**, *255*, 3472.
(13) Clarke, M. J.; Dowling, M. G.; Garafalo, A. R.; Brennon, T. F. *J. Am. Chem. Soc.* **1979**, *10*, 223.
(14) Sawyer, D. T.; Morrison, M. M. *J. Am. Chem. Soc.* **1978**, *100*, 211.
(15) Goodgame, M.; Johns, K. W. *Inorg. Chim. Acta* **1979**, *37*, L559.
(16) (a) Frey, C. M.; Stuehr, J. E. *J. Am. Chem. Soc.* **1978**, *100*, 134. (b) Frey, C. M.; Stuehr, J. E. *J. Am. Chem. Soc.* **1978**, *100*, 139. (c) Thomas, J. C.; Frey, C. M.; Stuehr, J. E. *Inorg. Chem.* **1980**, *19*, 501. (d) Thomas, J. C.; Frey, C. M.; Stuehr, J. E. *Inorg. Chem.* **1980**, *19*, 505. (e) Frey, C. M.; Stuehr, J. E. In "Metal Ions in Biological Systems"; Sigel, H., Ed.; Marcel Dekker: New York, 1974; Vol. I, p 51.
(17) Light, D. R.; Walsh, C.; Marletta, M. A. *Anal. Biochem.* **1980**, *109*, 87.
(18) Briggs, T. Ph.D. Thesis, Case Western Reserve University, 1976.
(19) Eigen, M.; DeMaeyer, L. *Tech. Org. Chem.* **1963**, *8*, 895.
(20) The exact wavelength depended on the concentrations of the solution and the indicator. Though the effect is similar with either indicator, CPR was usually found to give a much noisier signal than BCP; hence the latter was used for most of the work with indicator.

0002-7863/86/1508-0820$01.50/0

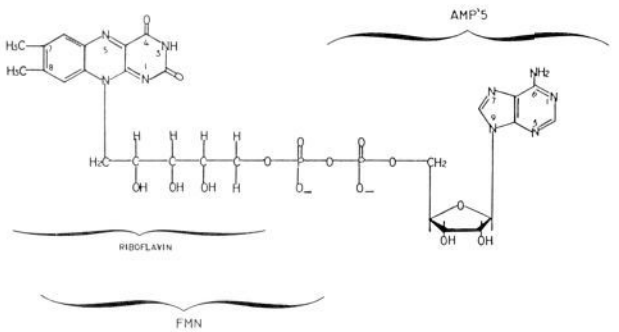

Figure 1. Structure of FAD, showing the relationship to the coenzymes FMN and AMP5′.

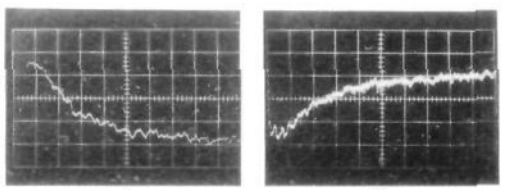

Figure 2. Typical oscilloscope traces (transmittance vs. time) showing the two relaxation times for NiFMN: 1.6×10^{-2} M Ni^{2+}, 4.62×10^{-3} M FMN, 5×10^{-4} M BCP at pH 5.83. (A) (fast effect) 100 μs/div; (B) (slow effect) 1 ms/div.

relaxations were monitored at 500–525 nm in the absence of indicator or at 572 or 614 nm in the presence of chlorophenol red or bromocresol green ($pK_{In} = 4.68$), respectively. Typically, three T-jump determinations were carried out for each solution. The uncertainties in the relaxation times were ±5–10%. The pH of each solution was measured at 15 °C by a Corning or Beckman combination electrode and was adjusted by adding KOH or HNO_3 from a 50-μL pipet.

The concentrations of ligand and metal ion ranged from 6×10^{-4} to 2×10^{-2} M for the FMN studies and 1.25×10^{-3} to 1.00×10^{-2} M for the FAD experiments. The ligand–metal ratio was near unity in most cases.

Treatment of Data. The titration data were analyzed by a computer program which tested for the various complexed species and calculated equilibrium concentrations. Changes in ionic strength which occurred during the course of titration were taken into account.[18] The pK_a's and binding constants thus obtained are listed in Table I.

For the NiFMN system, two relaxation times were detected and characterized as a function of pH and concentration. For NiFAD, we observed and characterized four separate relaxation effects. The latter were only slightly concentration- and pH-dependent.

NiFMN System

There are three ionizable protons on FMN: two on the phosphate group and a third on the isoalloxazine ring (N3) (Figure 1). The third proton ionization is far above the pH range of the present study, and the kinetic data were consistent with complexes formed from the ligand in which the N-3 remains protonated. In the context of the present work, then, L^{2-} is the free anionic form of the ligand, and HL^- has the secondary phosphate protonated. Values for the pK's and metal ion stability constants are shown in Table I. The K_{ML} value is larger than that for $NiRiPO_4$ (80 M),[21] which indicates an interaction of Ni(II) with the isoalloxazine ring even when the N3 is protonated.

Two relaxation effects, corresponding to transmittance changes in opposite directions, were observed in the kinetic experiments: one (τ_1) on the order of 0.2 ms; the other (τ_2) at about 2 ms. Figure 2 shows the two effects for one of the solutions. Both effects could be observed either with or without an indicator and were absent in solutions of only FMN or FMN plus indicator. However, the characteristics of the effects were such that the fast effect was best determined in the presence of the indicator, while the slow effect was easily observed at 505–530 nm without indicator. Concentrations and pH were adjusted so as to optimize one or the other of the two effects. As a result, most of the entries in

(21) Frey, C. M.; Stuehr, J. E. *J. Am. Chem. Soc.* **1972**, *94*, 8898.

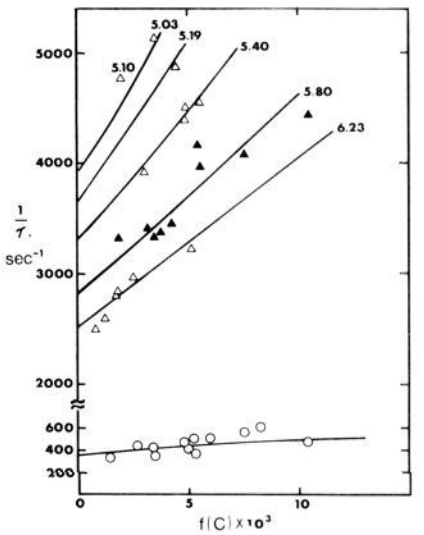

Figure 3. Concentration and pH dependences of the two relaxation times for the NiFMN system. Top: The variation of τ_1^{-1} with concentration at various pH values, as indicated. Bottom: The variation of τ_2^{-1} with concentration over the pH range 5.0–6.3. For both sets of curves, the solid lines are calculated from Scheme I.

Scheme I

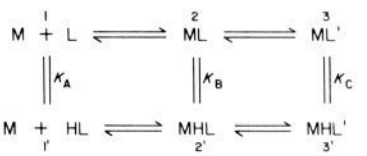

Table II (in supplementary material) show only one or the other of the two relaxation times even though both times were observed for virtually every solution.

The relaxation times were found to be dependent on the metal and ligand concentrations (see Figure 3). The behaviors of the two effects were different in detail. The variation of τ_2^{-1} with concentration or pH was very slight but detectable. On the other hand, τ_1^{-1} rises rapidly with increasing concentration and, for solutions of the same metal and ligand concentration, increases with increasing hydrogen ion concentration. The change in τ_1 with pH for any one solution was clearly discernible.

The detailed concentration and pH dependencies of τ_1 and τ_2 are quite similar to those for the relaxation times found earlier in the nickel ribose phosphate and NiAMP systems, respectively.[16c,d] The mechanism proposed for the latter involves a dual-pathway, back-bound complex mechanism, shown schematically in Scheme I. In this scheme, M and L represent the free metal and ligand ions, ML the complex in which the metal ion is bound to the phosphate moiety, and ML′ the complex involving simultaneous interaction with the phosphate and adenine moieties. The bottom row shows the corresponding complexes with the ligand protonated at the secondary phosphate. The slow complexation steps are shown by arrows, the rapid proton transfers by = signs.

We find the two relaxation times observed in the NiFMN system to correspond to the two predicted times $\tau_\pm$ for Scheme I. The only difference is that the species ML′ and MHL′ now correspond to the simultaneous interaction of Ni(II) with the phosphate and *isoalloxazine* moieties. The two relaxation times are given by eq 1 where a_{ij} are fairly complicated functions[16d] of the rate constants and equilibrium concentrations of species in Scheme I. The two roots τ_+ and τ_- from eq 1 correspond to the

$$\frac{1}{\tau_\pm} = \frac{(a_{11} + a_{22})}{2}\left(1 + \left[1 - \frac{4(a_{11}a_{22} - a_{12}a_{21})}{(a_{11} + a_{22})^2}\right]^{1/2}\right) \qquad (1)$$

measured τ_1 and τ_2 values. Of the equilibrium constants in Scheme I, K_{23} and K'_{23} are calculated from the relationships K_{ML}

Table III. Kinetic Data for the Interaction of Ni(II) with FAD[a]

$10^3[M]^0$, M	$10^3[L]^0$, M	pH[b]	τ_{exptl}^{-1}, s^{-1}	τ_{calcd}^{-1}, s^{-1}	$10^3[M]^0$, M	$10^3[L]^0$, M	pH[b]	τ_{exptl}^{-1}, s^{-1}	τ_{calcd}^{-1}, s^{-1}
10.0	10.0	6.10	(1) 9900	10538	2.5	2.5	6.30	(1) *c*	9831
			(2) 350	295				(2) 280	268
			(3) 200	237				(3)	234
			(4) 29	30				(4) *c*	20
10.0	10.0	6.00	(1) *c*	10537	2.5	2.5	6.20	(1)	9830
			(2) *c*	295				(2) 290	268
			(3) 235	237				(3)	234
			(4) 31	30				(4)	20
10.0	10.0	5.80	(1) 9800	10537	2.5	2.5	6.10	(1) 9760	9830
			(2) 345	295				(2) 330	268
			(3) 220	237				(3) *c*	234
			(4) 30	30				(4)	20
10.0	10.0	5.10	(1) 11100	10530	2.5	2.5	5.80	(1) *c*	9830
			(2) 280	295				(2) 280	268
			(3) 230	237				(3) *c*	234
			(4) *c*	30				(4)	20
10.0	10.0	5.00	(1) 11000	10527	2.5	2.5	5.10	(1) *c*	9824
			(2) *c*	295				(2) 240	268
			(3)	237				(3) *c*	234
			(4)	30				(4) 19	20
10.0	10.0	4.90	(1)	10525	2.5	2.5	4.90	(1)	9821
			(2) 290	295				(2) 260	268
			(3) 250	237				(3)	234
			(4)	30				(4) 21	20
10.0	10.0	4.50	(1)	10507	2.5	2.5	4.50	(1) *c*	9808
			(2) 290	295				(2) 250	267
			(3) 240	237				(3)	234
			(4)	30				(4) *c*	20
5.0	5.0	6.10	(1) 9690	10113	1.25	1.25	6.10	(1) *c*	9650
			(2) 310	279				(2) 290	262
			(3) 250	236				(3)	232
			(4)	25				(4) *c*	17
5.0	5.0	5.80	(1) 11800	10112	1.25	1.25	5.90	(1)	9650
			(2) 370	279				(2) 280	262
			(3) 240	236				(3)	232
			(4)	25				(4)	17
5.0	5.0	5.10	(1) *c*	10106	1.25	1.25	5.80	(1) *c*	9650
			(2) 250	278				(2) 330	262
			(3) 240	236				(3) *c*	232
			(4) 26	24				(4) *c*	17
5.0	5.0	4.50	(1) *c*	10085	1.25	1.25	4.60	(1) *c*	9636
			(2) 230	278				(2) 230	262
			(3) 240	236				(3)	232
			(4)	24				(4)	17
5.0	5.0	4.40	(1)	10079	1.25	1.25	4.50	(1)	9633
			(2) 265	277				(2) 220	261
			(3)	236				(3)	232
			(4)	24				(4)	17

[a] 15 °C, I = 0.1 N KNO_3. [b] a_H values converted to $[H^+]$ with γ_H = 0.83. [c] Effect observed but not characterized.

$= K_{12}(1 + K_{23})$ and $K_{MHL} = K'_{12}(1 + K'_{23})$, where K_{ML} are thermodynamically measured equilibrium constants. In addition, K_B and K_C are fixed by circular relationships among the constants. As a consequence, the only unknowns are the four forward rate constants in Scheme I and the two equilibrium constants for the phosphate interactions, K_{12} and K'_{12}. All best-fit constants were determined via a nonlinear regression technique.[22] The results are given in Table IV.

Figure 3 shows the experimental points as a function of pH and concentration for the two relaxation effects and the theoretical lines calculated from eq 1. At a given pH, τ_1^{-1} varies linearly with concentration. The slopes of the lines correspond to the "effective" forward rate constant k_{1f} which is constant at a given pH.

$$k_{1f} = k_{12} + k'_{12}K_A[H] \quad (2)$$

Equation 2 predicts that the slopes should increase linearly with the hydrogen ion concentration; this prediction is verified by experiment. This behavior is exactly that found earlier for the $NiRiPO_4$ system,[16c] and the present values of k_{12}, k'_{12}, and K_{12} agree very well with those for $NiRiPO_4$ (Table IV).

Scheme I, with the rate constants in Table IV, predicts only a small dependence of τ_2 upon concentration or pH. Figure 3 shows that a single curve reproduces all the data over the pH range 5.1–6.2. The same mechanism predicts for AMP5′ a strong pH dependence; the difference in behavior is due principally to the considerably smaller k_{23} and k'_{23} values for FMN compared to AMP. As a consequence, the slow process for the former is relatively "decoupled" from the faster process and is much less pH- and concentration-dependent.

NiFAD System

There are four ionizable protons on FAD, two on the phosphate bridge in the ribityl chain, a third on the adenine ring, and a fourth on the isoalloxazine ring (N3) (Figure 1). Values were obtained for three of these pK's. It is important to note that all pK values are either well above or below the pH range of our study. Therefore L^{2-} represents the species in which both phosphate groups and the adenine ring are deprotonated.

Four separate relaxation effects ($\tau_1 - \tau_4$) were characterized for the NiFAD system; the relaxation times ranged from 90 μs to 33 ms. The pH dependences for all effects were negligible; the variations shown in Table III are probably within experimental error. The relaxation time τ_2 alone demonstrated a small but definite concentration dependence. In most instances, it was not possible to accurately determine all four relaxation times for a given solution. We wish to emphasize however that all four effects

(22) Feltch, S. Ph.D. Thesis, Case Western Reserve University, 1980.

Table IV. Rate and Equilibrium Constants[a] for the Interaction of Ni(II) with FAD, FMN, AMP, and $RiPO_4$

	NiFAD	NiFMN	NiAMP5'[b]	$NiRiPO_4$[c]
		Phosphate Complexes		
K_{12}, M^{-1}	25 ± 5	72.6 ± 0.5	80	80
$10^{-5}k_{12}$, M^{-1} s^{-1}	2.0 ± 0.5	1.47 ± 0.16	2.3 ± 0.1	1.4
k_{21},[d] s^{-1}	8000	2025	2870	1810
		Phosphate–Adenine Ring Complexes		
K_{25}	3.0 ± 0.5		4[e]	
k_{25}, s^{-1}	550 ± 75		1510 ± 50[e]	
k_{52}[d] s^{-1}	183		380[e]	
		Phosphate–Isoalloxazine Complexes		
K_{23}	0.62 ± 0.1	0.62		
k_{23}, s^{-1}	130 ± 20	246 ± 58		
k_{32}[d] s^{-1}	210	390		
		Phosphate–Adenine–Isoalloxazine Complexes		
K_{34}	18.2			
K_{54}	3.8			
k_{54}, s^{-1}	50 ± 20			
k_{45},[d] s^{-1}	13			
k_{34}, s^{-1}	30 ± 30			
k_{43},[d] s^{-1}	1.6			

[a] At 15 °C and I = 0.1 M KNO_3. [b] Reference 16d. [c] Reference 16c. [d] Value calculated from the forward rate constant and the equilibrium constant. [e] In reference 16c, this step is numbered 2–3.

were usually *detected*, even though some of the relaxation amplitudes were too small for accurate determination. This is indicated in Table III.

The fastest and slowest effects, designated as (1) and (4), respectively, could be observed both with and without indicator. The amplitudes of these effects decreased dramatically with decreases in pH and/or concentration. The faster effect, τ_1, had reciprocal relaxation times in the range of 9000–11 000 s^{-1}. This is consistent with the predictions for the interaction with the phosphate moiety alone and is comparable in magnitude to previously characterized $NiPO_4$ interactions.[16c,d]

Effects (2) and (3) were both found in the 2–3-ms time region. However, effect (2) could be observed only with indicator and, as mentioned, demonstrated a small concentration dependence: τ_2^{-1} ranged from approximately 250 to 345 s^{-1} over the range 1.25 × 10^{-3} to 1.00 × 10^{-2} M. This was the only effect that could be clearly observed over the entire pH and concentration range tested. Effect (3) was observed in the absence of indicator and demonstrated both a pH and concentration *independence*, with a relaxation value of approximately 240 s^{-1}.

We are well aware of the similarities in the values of τ_2 and τ_3, and the question of whether these are indeed two distinct relaxation effects must be addressed. This was investigated in some detail. In early work in this system, we proceeded on the basis that there were only three relaxation times. As work continued, however, experimental evidence forced us to conclude that there were two closely spaced relaxation times observable under different conditions. This evidence included the fact that the concentration dependence of τ_2 was always clearly observable. A solution without indicator *always* demonstrated a concentration-independent relaxation effect. When indicator was added to the indicator-free solution and the observation wavelength changed appropriately, the relaxation time shifted from τ_3 to τ_2.

Not only does the experimental evidence point to four distinct relaxation times, but in hindsight one would predict the existence of two closely spaced relaxation effects based on the presence of AMP and FMN in this dinucleotide (see Figure 1). Both mononucleotides individually yielded slow relaxation effects with nickel in the time region in question (this work and ref 16d). They also were observable with or without indicator, depending on the mononucleotide. The slower relaxation effect τ_4 is unique to the NiFAD system.

The absence of a strong pH and/or concentration dependence in the relaxation data usually makes it difficult to make definite mechanistic conclusions. However, there are several observations with which any proposed mechanism for this system should be consistent:

Scheme II

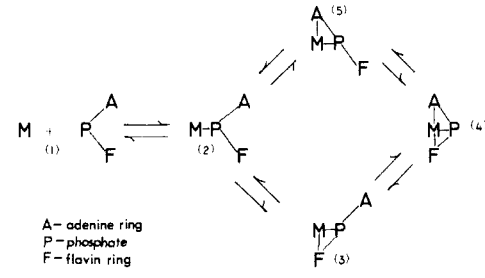

(1) Multiple (four) relaxation effects are observed for the experimental system, indicating the existence of (at least) four independent steps.

(2) The fastest relaxation time has values (~10^{-4} s) comparable to those in other Ni–phosphate systems.[16a,d] The middle two relaxation times are numerically similar to the slower times previously observed in NiAMP and NiFMN. The slowest relaxation process ($\tau_4^{-1} \approx 30$ s^{-1}) is unique to the NiFAD system.

(3) There is little to no pH dependence for these relaxation effects, indicating that protonated ligand reaction paths are not important in the pH range investigated.

(4) Some of these effects can be seen both with and without indicator; one effect can be seen only with indicator, one only without. In the NiAMP system, the relaxation effect could be followed only with indicator, whereas in the NiFMN study the reaction could be followed both with and without indicator. That is, the behavior observed in NiFAD is qualitatively and quantitatively similar to steps previously characterized in mononucleotide systems.

(5) We have already shown that for both of the mononucleotides AMP[16d] and FMN (this study), Ni(II) initially bonds with the phosphate group, followed by an interaction with its specific base ring.

(6) It is known that FAD is a rather flexible molecule and prefers a folded structure with the adenine and isoalloxazine rings stacked 3.5–4.0 Å apart and their long axes perpendicular to each other.[24]

Based on these considerations, we propose that in the $Ni^{II}FAD$ system, the metal initially binds to the phosphate oxygens (approaching the folded structure from the back) and then interacts with the adenine and isoalloxazine rings, first individually and

(23) Walaas, E. *Acta Chem. Scand.* **1958**, *12*, 528.
(24) (a) Frey, C. M.; Banyasz, J.; Stuehr, J. E. *J. Am. Chem. Soc.* **1972**, *94*, 9198. (b) Banyasz, J.; Stuehr, J. E. *J. Am. Chem. Soc.* **1973**, *95*, 7226.

then simultaneously. The tendency of the molecule toward folded conformations should facilitate the simultaneous interaction.

This mechanism is shown in Scheme II. It quantitatively accounts for both the number and behavior of all relaxation effects observed in this system where F, P, and A refer to the flavin, phosphate, and adenine moieties of FAD, respectively (Figure 1). (For simplicity, the various complexes will be abbreviated as C_2...C_4, corresponding to the numbered species in Scheme II.) The first complex C_2 involves metal ion binding to the phosphate oxygens only, followed by C_3, where both the flavin and the phosphate interact with nickel. The complex C_4 shows the metal bound to both rings as well as the phosphate groups, whereas in C_5 nickel is bound only to the adenine ring and phosphate.

The resulting four, first-order (close to equilibrium) differential equations are

$$d\delta C_2/dt = k_{12}[L]\delta M + k_{12}[M]\delta L + k_{52}\delta C_5 + k_{32}\delta C_3 - (k_{21} + k_{25} + k_{23})\delta C_2$$

$$d\delta C_3/dt = k_{23}\delta C_2 - (k_{32} + k_{34})\delta C_3 + k_{43}\delta C_4$$

$$d\delta C_4/dt = k_{34}\delta C_3 - (k_{45} + k_{43})\delta C_4 + k_{54}\delta C_5$$

$$d\delta C_5/dt = k_{25}\delta C_2 + k_{45}\delta C_4 - (k_{54} + k_{52})\delta C_5$$

All concentration variables except four may be eliminated by the use of mole balance relationships involving M, L, H^+, and the preequilibrium relationships involving the rapid proton-transfer reactions, thus yielding the fourth-order determinant

$$\begin{vmatrix} a_{11} - \frac{1}{\tau} & a_{12} & a_{13} & a_{14} \\ a_{21} & a_{22} - \frac{1}{\tau} & a_{23} & a_{24} \\ a_{31} & a_{32} & a_{33} - \frac{1}{\tau} & a_{34} \\ a_{41} & a_{42} & a_{43} & a_{44} - \frac{1}{\tau} \end{vmatrix} = 0$$

where the a_{ij} coefficients are

$$a_{11} = -k_{12}([M]^* + [L]) - (k_{21} + k_{25} + k_{23})$$

$$a_{12} = -k_{12}([M]^* + [L]) + k_{32}$$

$$a_{13} = -k_{12}([M]^* + [L]);\ a_{14} = -k_{12}([M]^* + [L]) + k_{52}$$

$$a_{21} = k_{23};\ a_{22} = -(k_{32} + k_{34});\ a_{23} = k_{43};\ a_{24} = 0$$

$$a_{31} = 0;\ a_{32} = k_{34};\ a_{33} = -(k_{45} + k_{43});\ a_{34} = k_{54}$$

$$a_{41} = k_{25};\ a_{42} = 0;\ a_{43} = k_{45};\ a_{44} = -(k_{54} + k_{52})$$

where * indicates division by $1 + \beta$ and

$$\alpha = [In]/(K_{In} + [H])$$

$$\beta = [H]/[K_a + [L]/(1 + \alpha)]$$

$$K_{In} = [H][In]/[HIn];\ K_a = [H][L]/[HL]$$

This determinant generates a fourth-order polynomial, the roots of which are the negative reciprocals of the four relaxation times for this mechanism.

Although there are 15 quantities in this scheme (10 rate constants and 5 equilibrium constants), 5 rate constants can be eliminated via the appropriate equilibrium expressions. Two of the equilibrium constants are fixed by the following identities:

$$K_{ML} \equiv K_{12}[1 + K_{23} + K_{25} + (K_{25}K_{54})]$$

$$K_{34} \equiv (K_{54}K_{25})/K_{23}$$

As a consequence, five rate constants and three equilibrium constants remain to be determined. This did not pose a serious problem since we had observed 42 relaxation times for 24 different solutions. In addition, in initial computer iterations, we set certain rate constants equal to the corresponding values previously determined for the AMP and FMN systems, i.e., k_{12} and K_{12}, k_{23} and K_{23}, and k_{25} and K_{25}, which correspond to the metal/phosphate, the metal/isoalloxazine ring, and the metal/adenine ring interactions, respectively (ref 16d and this work).

A literature value for K_{ML} for the Ni^{2+} complex was not available. Walaas[23] had shown that K_{ML} for several other transition-metal ions was approximately 200–300 M^{-1}. Our own attempts to determine K_{ML} spectroscopically were consistent with a value of this magnitude within rather large error limits; as a consequence, K_{ML} was set equal to 250 M^{-1}. The quality of fit of the kinetic data was not particularly sensitive to its value.

A computer program was used to vary the unknown parameters so as to yield a best fit between experiment and data. Table III shows both τ_{exptl}^{-1} and τ_{calcd}^{-1}. A grid search was used to generally map out the eight-dimensional χ^2 surface. The eight unknowns were then varied systematically to determine the best fit to the data over the entire pH and concentration range tested. In mapping the χ^2 surface, we observed that virtually all the constants had a very narrow range of values that would reproduce the experimental data. The effect of manipulating one rate constant is primarily manifested in the change of value of one relaxation time. For example, k_{12} (the rate constant for the phosphate interaction) was strongly coupled to τ_1, k_{25} (the adenine ring interaction) to τ_2, and k_{23} (the flavin ring interaction) to τ_3. As a consequence, we were able to determine these rate constants with considerable certainty.

Table IV shows the best fit constants for NiFAD and compares them to those for NiFMN, NiAMP, and $NiRiPO_4$.

Discussion

The two systems FMN and FAD are interesting in that they are structurally related and consist in part of compounds we have characterized in previous reports.[16c,d] The multiple relaxation effects in FAD, on the other hand, and the strong pH dependence exhibited by FMN are entirely consistent with their known structure and ionization properties.

There follows a brief discussion and, where appropriate, a comparison of each of the interactions with Ni^{2+} in the two systems.

Phosphate Interaction (Step 1–2 in Schemes I and II and Step 1′–2′ in Scheme I). The rate constants for the binding of Ni^{2+} to the phosphate group are the same, within probable uncertainties, for FMN and FAD, as well as for AMP and ribose phosphate (Table IV). The rate constant k_{1p} for the penetration of the ligand (phosphate) into the inner coordination sphere of the metal ion may be calculated from $k_f = K_{os}k_{1p}$ where k_f is the forward rate constant and K_{os} is the outer-sphere equilibrium constant for the conditions of the experiment. We have estimated[24] K_{os} to be 10 and 2 M^{-1} for charge types of 2–2 and 2–1, respectively at I = 0.1. The fact that the phosphate overall rate constants (k_{12} and k'_{12}) are the same for the various systems naturally leads to the same ligand penetration rate constants, as shown in Table IV. We conclude that the rate-determining step in all cases is the displacement of one or more water molecules from the primary coordination sphere of the metal ion.

The equilibrium constant for the step 1–2 is smaller for NiFAD by a factor of 3 compared to the other systems. This is a consequence of the fact that the binding site is a terminal phosphate in the other three systems; in FAD, the metal ion interacts with two separate phosphate groups, each with a single proton pK of about 2. The various reverse rate constants simply reflect the difference in binding strengths.

Isoalloxazine and Adenine Ring Interactions (Step 2–3 in Schemes I and II and Step 2–5 in Scheme II, Respectively). Within experimental error, the binding constant K_{25} is the same for NiFAD and NiAMP, and K_{23} is the same for NiFAD and NiFMN. The *rate constants* for these steps are considerably smaller (by a factor of 2–3) for NiFAD compared to the other systems. We believe that this result reflects the conformational properties of FAD in solution. This ion exists predominantly in a folded conformation[25] such that the two ring systems interact (Scheme II and Figure 1). The fastest step is the binding of the metal ion to the phosphate group. In order to further interact with either of the ring systems in FAD, the metal ion must disturb

(25) Kainosho, M.; Kyogoka, Y. *Biochemistry* **1972**, *11*, 741.

the folded structure that predominates in solution. This is reflected in the reduced rate constants.

Phosphate–Adenine–Isoalloxazine Complex (Steps 3–4 and 5–4 in Scheme II). Structure 4 in Scheme II involves simultaneous interactions with the phosphate moiety and adenine and isoalloxazine ring systems. This complex is of course unique to the NiFAD system and corresponds to τ_4 in Table III. Presumably, the complex is folded back upon itself, in a manner opposite to that in the free coenzyme. Space-filling models demonstrate the flexibility of the FAD molecule and clearly show the possibility of the 3-fold interaction.

In principle, there are two routes by which the complex C_4 can be formed: 3–4 and 5–4. Experimentally, we found the relaxation time τ_4 for Scheme II to be relatively insensitive to step 3–4. A rate constant $k_{34} = 30\ s^{-1}$ was the best-fit value from the computer analysis, but values of 60 or even 0 s^{-1} did not give markedly inferior fits. The rate constants for this step are essentially indeterminate.

On the other hand, the mechanism was quite sensitive to the value of the rate constant k_{54}. Since this step does not exist in the other systems, the rate constants cannot be compared with other values. It is not surprising, however, that step 5–4 is the slowest of the four that have been characterized for NiFAD.

Conclusions and Significance

In conclusion, we have shown that Ni(II) interacts with FMN in a manner analogous to AMP5′. That is, two concentration-dependent relaxation times in the 10^{-4}–10^{-3}-s time region were observed for each system. Rate constants were found to be comparable in the two systems for the phosphate and base interactions. For the NiFAD system, four separate relaxation times were characterized. A multistep mechanism involving a phosphate interaction followed by interactions with the individual components of the coenzyme was found to be consistent with the data. To the best of our knowledge, no other binary system has been observed with four relaxation times.

There could well be some biological importance in the fact that metal ions form several different bound structures with FAD. A redox metal ion, for example, may be tightly bound to the phosphate moiety and simultaneously interact weakly with the isoalloxazine ring, keeping the metal in the proper spatial orientation and thus facilitating electron transfer. Finally, it is evident that simple model experiments designed to demonstrate metal–flavin interactions in biological systems must take into account the fact that the strongest interaction is with the phosphate moiety.

Acknowledgment. This work was supported by the NIH in the form of a research grant to J.E.S. (GM-13,116). J. B. gratefully acknowledges support from the B. F. Goodrich Corp. in the form of a graduate fellowship. We thank Dr. Steven Feltch for his assistance with the computer analyses.

Registry No. FAD, 146-14-5; FMN, 146-17-8; Ni, 7440-02-0.

Supplementary Material Available: Kinetic data for the interaction of Ni(II) with FMN (Table II) (2 pages). Ordering information is given on any current masthead page.

Compatibility of β- and γ-Turn Features with a Peptide Backbone Modification: Synthesis and Conformational Analysis of a Model Cyclic Pseudopentapeptide

Arno F. Spatola,*† Mohmed K. Anwer,† Arlene L. Rockwell,‡ and Lila M. Gierasch*‡

Contribution from the Department of Chemistry, University of Louisville, Louisville, Kentucky 40292, and the Department of Chemistry, University of Delaware, Newark, Delaware 19711. *Received March 11, 1985*

Abstract: A backbone-modified cyclic peptide has been synthesized and characterized by carbon-13 and proton NMR spectroscopies, and the results have contrasted with well-defined parent all-amide model cyclic pentapeptide. The pseudopeptide was prepared by solid-phase methods using two different linear sequences and then cyclized to yield a common structure. When a mixture of diphenylphosphoryl azide, hydroxybenzotriazole, and (dimethylamino)pyridine was used, the yield of cyclization was 85%. The pseudopeptide, cyclo[Gly-Proψ[CH_2S]Gly-D-Phe-Pro], containing a single thiomethylene group as an amide bond surrogate was nevertheless able to adopt both β- and γ-intramolecular hydrogen bonds in deuteriochloroform, as assessed by diagnostic chemical shift, temperature dependence, and solvent dependence data. However, in contrast to its all amide counterpart, the cyclic pseudopeptide showed evidence of *cis/trans*-proline peptide bond isomerism upon addition of dimethyl sulfoxide.

Variation of backbone elements in peptides can be expected to have profound consequences on conformation, secondary structure, and solubility as well as on biologically important factors such as receptor selectivity, altered transport properties, and different patterns of enzymatic degradation.[1] Reported peptide backbone changes have included not only configurational (*R,S*) interchanges, but also N^2 and C alkylations,[3,4] dehydroamino acids,[5] α-carbon substitutions ("aza" analogues),[6] and an increasing variety of amide bond replacements (surrogates). In the latter category are such amide substitutions as ψ[COO] (depsipeptides),[7] ψ[NHCO] (retroamides),[8] ψ[CSNH],[9] ψ[CH_2NH],[10] ψ[$COCH_2$],[11] ψ[NHCONH],[12] ψ[CH=CH],[13] and ψ[CH_2S][14] functionalities.

†University of Louisville
‡University of Delaware

(1) Spatola, A. F. "Chemistry and Biochemistry of Amino Acids, Peptides and Proteins"; Weinstein, B., Ed.; Marcel Dekker: New York, 1983; Vol. 7, pp 267–357.
(2) Hall, M. M.; Khosla, M. C.; Khairallah, P. A.; Bumpus, F. M. *J. Pharmacol. Exp. Ther.* **1974**, *188*, 222.
(3) Jones, D. S.; Kenner, G. W.; Preston, J.; Sheppard, R. C. *J. Chem. Soc.* **1965**, 6227.
(4) Khosla, M. C.; Stachowiak, K.; Smeby, R. R.; Bumpus, F. M.; Pirui, F.; Lintner, K.; Fermandjian, S. *Proc. Natl. Acad. Sci. U.S.A.* **1981**, *78*, 757.
(5) Stammer, C. H. "Chemistry and Biochemistry of Amino Acids, Peptides, and Proteins"; Weinstein, B., Ed.; Marcel Dekker: New York, 1982; Vol. 6, p 33.

0002-7863/86/1508-0825$01.50/0